Simulation and Related Experimental Validation of Acetic Acid/Water Distillation Using *p*-Xylene as Entrainer

Carlo Pirola,*[,†] Federico Galli,[†,‡] Flavio Manenti,[‡] Michele Corbetta,[‡] and Claudia L. Bianchi[†]

[†]Dipartimento di Chimica, Università degli Studi di Milano, via Golgi, 19, 20133 Milano, Italy

[‡]Dipartimento CMIC "Giulio Natta", Politecnico di Milano, piazza Leonardo da Vinci 32, 20133 Milano, Italy

1. INTRODUCTION

The recovery of acetic acid from aqueous solutions is an important operation, among others, in the cellulose acetate industry and in the terephthalic and isophthalic acid production processes.[1−5] The acetic acid and water system does not show an azeotrope at atmospheric pressure but shows a tangent pinch on the pure water end. For this reason, the separation of this mixture by direct distillation is not technically feasible. The addition of a third component, generally immiscible with water, allows the separation of water and acetic acid by heterogeneous azeotropic distillation, as reported in the literature.[6,7] Water is entrained by the third component to the head of the column while acetic acid leaves the column from the bottom, mixed with the entrainer from which it must be purified before being recycled.

Different kinds of entrainers have been proposed for this separation: ethyl acetate,[8,9] *n*-butyl acetate,[10−13] vinyl acetate,[14] or iso-butyl acetate.[12,15] A comparison study using ethyl acetate, iso-butyl acetate, or *n*-butyl acetate was reported by Chien.[16] These entrainers are efficient in recovering acetic acid from water but are potential contaminants when acetic acid has to be recycled to the main production process. The use of *p*-xylene as entrainer is here proposed with particular reference to the industrial terephthalic acid production.[1] This process is well described by Li.[10] *p*-Xylene can work as water entrainer and can be directly recyclable with acetic acid to the catalytic reactor without further purification because it is the principal raw material in the terephthalic acid production process. The main advantages in using *p*-xylene in comparison with other entrainers are (a) no need for the purification of the acetic acid/*p*-xylene mixture and (b) having a component not involved and therefore potentially contaminating the terephthalic production process. This solution has been proposed in a recent paper by Wang[17] and compared with the traditional entrainer butyl acetate. In this last paper, particular attention was devoted to the control strategy of the distillation plant, while in the present paper a detailed study of both the phase equilibria of the ternary system and the experimental distillation separation results are reported.

In a previous paper,[18] with the aim of using a predictive model, UNIFAC together with the Hayden−O'Connel[19] correlation was adopted to model this ternary system. The fugacity coefficient was accounted for because the UNIFAC model alone was unable to correctly predict the fluid phase equilibria of the ternary mixture. In this work, in contrast, the UNIQUAC[20] activity model was adopted for the calculation of the activity coefficients and the acetic acid association was considered negligible, due to both the temperature inside the column and the acetic acid dilution in the mixture, as discussed in detail in the following. We decided to change the thermodynamic model because the availability of experimental data, coupled with a robust regression tool, allowed us to obtain a more reliable model with respect to the previous predictive one, considering also that in the previous work[18] the fugacity coefficients were accounted for because of the poor fitting of the UNIFAC model predictions. In this work, UNIQUAC binary parameters were regressed using the robust optimizer belonging to the BzzMath library starting from these considerations and taking into account different experimental equilibrium data available in literature. These data concern both the ternary system[21] and the binary mixtures involved.

The validity of the proposed thermodynamic model, together with the possibility of using *p*-xylene as entrainer, was proven by simulating two kinds of experiments performed on this ternary mixture: evaporation runs using a batch distillation apparatus and distillation column runs (15 trays, 5 m height) made at different operating conditions to perform continuous heterogeneous

Received: July 10, 2014
Revised: October 27, 2014
Accepted: October 28, 2014
Published: October 28, 2014

azeotropic distillation. The overall tray efficiency of the column was estimated and discussed.

2. EXPERIMENTAL SECTION

The following abbreviations will be used in the paper: W for water, AcAc for acetic acid, and *p*-xyl for *p*-xylene. Compositions will be expressed in term of liquid molar fraction, x_i, or vapor molar fraction, y_i, where i = W, AcAc, or *p*-xyl. If the compositions are referred to a particular stream (F, feed of the mixture W/AcAc; dist, distillate; res, residue), these labels will be inserted. For example, the molar fraction of acetic acid in the distillate will be $x_{dist,AcAc}$.

AcAc and *p*-xyl were used as received from Aldrich (purity >99.9%) without further purification; water was bidistilled.

Nine experimental runs were carried out in two different apparatus. Runs labeled as run 1−3 were performed in a batch distillator with a reboiler of 0.1 L, loading three different mixtures of W, AcAc, and *p*-xyl at different compositions (reflux ratio = 0); the condensed vapors were sampled every 5 min.

Runs labeled as run 4−9 were performed in a Pyrex Bubble-cap tray micropilot column plant (Normschliff, control unit Mod. DEST-STAR IV).

The height of this column is 5000 mm for a total of 15 trays; it is thermally insulated by a vacuum gap and through a silver shield. The plate diameter is 50 mm, the tray space 60 mm, the downcomer area 200 mm^2, the operating hold-up per plate 11 mL, and the residual hold-up per plate 0.8 mL.

The reboiler at the bottom has a capacity of 2 L. The resulting thermal loss was about 850 kJ h^{-1}, which is approximately 30% of the total exchanged heat, and this was accounted for in all simulations. During the simulations, a pressure drop of 15 kPa per tray was adopted.[22] The reflux in the column was set similarly to a Todd column, i.e., using a valve whose opening (reflux equal to 0) and closing (total reflux) were regulated by a timer. Both the condensed phases were refluxed in the column during the experiments performed at finite reflux. Runs were carried out using different operative configurations. Runs 4−5, at total reflux, were used to estimate the global efficiency of the column. The liquid compositions in the reboiler and at the top of the column and the vapor composition of tray number 12 (from the top tray) were experimentally determined. In runs 6 and 7, the mixture W/AcAc was fed at tray number 12 while the entrainer (*p*-xyl) at tray number 2 (top of the column). In run number 8, the mixture W/AcAc was fed into the reboiler and the entrainer at the tray number 2 to reproduce only the rectification part of the whole column. Finally, in run 9, the mixture W/AcAc was fed at tray number 2 together with the entrainer to reproduce only the stripping part of the whole column. All the experimental runs were repeated at least three times, and the average values are reported.

Water content in the samples was determined by Karl Fischer titration; low acetic acid content (<2%$_{wt}$) was determined by titration using KOH 0.1 M and phenolphthalein as indicator. The AcAc and *p*-xyl concentration of all the samples was determined by gas chromatography using a GC 8000 series Fisons, equipped with a SE52 column (0.53 μm × 25 m). The optimized temperature program included a first isothermal step at 45 °C for 2 min and then a thermal increase up to 110 °C at 20 °C min^{-1}.

The simulations were carried out using PRO/II software version 9.1 by Simulation Science (SimSci-Esscor, Schneider Electric). The PRO/II-Excel add-on ternary_VLE of PRO/II was used for generating equilibria phase diagrams and distillation curves to compare with the experimental data. The computer algorithm used for the micropilot simulations was the PRO/II CHEMDIST VLLE, which is able to cope with both a single- and a double-liquid phase mixture, choosing in each case the appropriate set of parameters.

UNIQUAC parameters were regressed by the robust BzzMath optimizer.[23,24]

3. THERMODYNAMIC ASPECTS

The vapor pressures of W, AcAc, and *p*-xyl were calculated using the extended Antoine equation with the parameters of the PRO/II database, valid in the entire range of experimental temperatures (between 100 and 138 °C).

The normal boiling temperatures that characterize the W/AcAc/*p*-xyl system are those of the pure components (i.e., 100, 118, and 138 °C, respectively) and those of the two binary azeotropic binary mixtures, reported in Table 1 together with the compositions.

Table 1. Normal Boiling Temperatures and Azeotropic Composition of the Mixtures AcAc/*p*-xyl and W/*p*-xyl[25] and Calculated Values Using the UNIQUAC Activity Coefficient Model

	experimental data		calculated by UNIQUAC	
system	T (K)	$x_{p\text{-xyl}}$	T (K)	$x_{p\text{-xyl}}$
AcAc/*p*-xyl	388.25	0.18	388.25	0.20
W/*p*-xyl	365.7	0.24	365.54	0.24

The fluid phase equilibria data available in the literature concerning W, AcAc, and *p*-xyl[21,25−28] have been used to estimate the activity coefficients using the UNIQUAC activity model, in accordance with literature reports on similar systems.[29,30] An important aspect of the studied system concerns the association of AcAc molecules to give dimers and tetramers in the vapor phase. In the literature different approaches are used to interpret this phenomenon. For example, Chien[16] uses the Hayden−O'Connel correlation,[19] working on the second virial coefficient for the calculation of the AcAc fugacity coefficient, whereas Chengfei[31] prefers not to consider the acetic acid association. Another interpretation, used for reactive distillation units, is given by Horstmann[29] for whom it is not necessary to calculate the fugacity coefficient, but the AcAc dimerization in the vapor phase is considered with the Marek and Standart equation.[32]

In the present work the proposed thermodynamic interpretation is based on the following considerations: (1) UNIQUAC activity model can represent conveniently this system, but a robust regression of the parameters is necessary because of the complexity of the mixture involved in the distillation column. (2) The fugacity coefficient can be supposed to be equal to 1 considering both the low pressure (atmospheric) used in this work and the hypothesis of very low AcAc association in the vapor phase at the experimental temperatures. This approach is the same as that of Horstmann.[29] The formation of the dimer molecules is not considered because the temperatures at which the column was operating are in the 92−138 °C range, and this means that the association constant (k_D, which depends exponentially on temperature) is very low. In fact, by considering the Marek and Standart equation,[32] increasing the temperature, for example from 20 °C until 120 °C, results in decreasing the k_D value by about 2500 times. Another important consideration is that the critical point for the separation of the W/AcAc system is

the zone in which AcAc molecules are very diluted in water, and then the actual contribution of acetic acid associated molecules could be neglected. This thermodynamic approach, very rigorous for the liquid activity calculation but simplified for what concerns the acetic acid association, can be very useful for obtaining a fast simulation of the system, limiting the computational cost. This last statement is particularly meaningful in a plant real-time analysis, where if the simulation convergence is reached faster, a better dynamic control could be possible. The hypothesis here discussed required the experimental validation reported in the following.

4. UNIQUAC PARAMETERS REGRESSION

UNIQUAC regression of the model parameters was performed by means of the set of robust optimizers belonging to the BzzMath library.[23]

Such optimizers are based on object-oriented programming and parallel computing so as to reduce the computational time.[33] This library possesses numerical methods able to simultaneously handle the so-called narrow-valley problem, which typically arises in the estimation of kinetic and thermodynamic parameters,[34] the possible multicollinearities which could be due to coupled chemical-physical phenomena, and the possible presence of bad quality measures with the identification of outliers.[35] The adopted formulation of the nonlinear regression problem[34] for the estimation of binary interaction parameters is based on the minimization of an objective function, subjected to the nonlinear system resulting from the equilibrium and stoichiometric equations.

The objective function is a weighed ($\omega_{j,k}$) least sum of square errors, in which $g_k(\mathbf{x}_j, \mathbf{b})$is the model prediction of the kth dependent variable, as a function of independent variables ($\mathbf{x}_j$) and model parameters ($\mathbf{b}$). In eq 1, the problem formulation for the regression of the UNIQUAC binary interaction parameters of the ternary (W/AcAc/p-Xyl) vapor−liquid−liquid equilibrium is reported. The first guess for binary interaction parameters estimation has been taken from simulator databanks. A sensitivity analysis on first guess values has confirmed the robustness of the optimizer.

$$\min_{\mathbf{b}} S(\mathbf{b}) = \sum_{j=1}^{N\text{exp}} \sum_{k=1}^{Ny} [\omega_{j,k}(y_{j,k} - g_k(\mathbf{x}_j, \mathbf{b}))]^2$$

$$\text{s.t.} \quad \text{Py}_i = P_i^o(T) x_{i,\text{aq}} \gamma_{i,\text{aq}}(T, \mathbf{x}_{\text{aq}}) \quad i = 1, 2, 3$$

$$x_{i,\text{aq}} \gamma_{i,\text{aq}}(T, \mathbf{x}_{\text{aq}}) = x_{i,\text{org}} \gamma_{i,\text{org}}(T, \mathbf{x}_{\text{org}}) \quad i = 1, 2, 3$$

$$\sum_{i=1}^{NC} x_{i,\text{aq}} = 1$$

$$\sum_{i=1}^{NC} x_{i,\text{org}} = 1$$

$$\sum_{i=1}^{NC} y_i = 1 \qquad (1)$$

Actually, the mistake made by some strategies implemented in commercial software[36−38] is to adopt search directions oriented along the bottom of the valley to find a step length within a line search framework. Such a search will prove ineffective because the direction is usually inexact and the valley is nonlinear. To exploit the search direction that inaccurately detects the bottom of the valley, it is necessary to change the point of view: (1) Any optimization algorithm can find the bottom of the valley by starting from a point outside the same valley. (2) The line joining two points on the bottom of the valley is a reasonable valley direction; therefore, there is a good probability that a point projected along such a direction will be close to the valley. (3) Nevertheless, this valley direction must not be used as the one-dimensional search direction, but rather as a direction along which a new point projection must be carried out. (4) This new point should not be discarded even though it is worse than the previous one; rather, it is the new starting point for a new search. (5) This search must be performed in the subspace orthogonal to the valley direction to prevent the issue of small steps arising. This philosophy is particularly simple in object-oriented programming. The optimization problem is split into two different levels:

1. The first level (outer optimizer) is managed by a single object that exploits the above-mentioned procedure to find a certain number, N, of points to initialize an even number of objects. N is 4 if the number of available processors is smaller than or equal to 4. N corresponds to the number of available processors otherwise.
2. In the second level (inner optimizer), each object uses a program to search for the minimum with a limited number of iterations starting from the point assigned by the outer optimizer.

This philosophy is useful in solving all problems demanding algorithm robustness: when the function (1) has many minima and we need to search for the global minimum, (2) has very narrow valleys (or steep walls), or (3) is undefined anywhere. All these problems arise in the estimation of thermodynamic parameters. Moreover, this philosophy is particularly effective when several processors are available. Actually, each object of the inner optimization can be managed by its dedicated processor.

Searching for the global optimum and tackling possible narrow valleys are both jobs for the outer optimizer. The following strategy is proposed to manage the N objects: three objects are required to apply the point projection, whereas the remaining $N - 3$ objects are selected by using the same techniques employed in optimal experimental design.[23] The outer optimizer collects initial and arrival points for each inner object and selects the two points between them that have the best performances. If these two points are very close to each other, the best third, fourth, ... is selected in place of the second to avoid any ill-conditioning while detecting the valley direction (Figure 1).

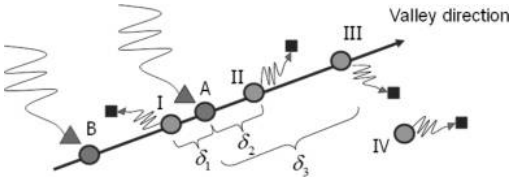

Figure 1. Robust C++ algorithm. Points A and B are on the bottom of the valley (A is the best one); points I, II, and III are the possible point projections along the valley direction. Point IV is placed out of the valley according to design of experiment techniques. The number of points out of the valley depends on the processors available.

Distances δ_1, δ_2, and δ_3 between points can be reduced or expanded depending on the results. For example, if point III results in a better inner optimum, distances are expanded. Points from the fourth to the *N*th are selected to have the farthest points compared to all the collected ones. This selection is efficiently carried out using techniques adopted and proven for the optimal design of experiments. The following procedure is adopted as the stop criterion. At each iteration, the number of points in the neighborhood of the optimum (given a tolerance value) is checked. If such a number is reasonable (according to an assigned value), a possible solution is reached. Theoretically, the number of points should be in the order of magnitude of the optimization problem dimensions, but it is preferable to use smaller numbers when the optimization size is large.

The inner optimizer has the task of quickly finding a local minimum or a point on the bottom of the valley even when robustness is required. It adopts different strategies explained elsewhere.[39] These strategies execute a search very limited in the amount of iterations because their target is to identify the bottom of the valley or the local minimum. The one-dimensional searches are carried out along the Cartesian axes and according to a specific priority: the first axis is the one with the smallest variation of the variable with respect to the valley direction of the previous iteration. The axis with the largest variation is not used.

The performance in terms of estimation accuracy has been proven with respect to the tools available in commercial suites. In fact, the regression of the binary VLLE interaction parameters is not possible using the PRO/II commercial tool because of the low set of experimental data.

The optimized parameters obtained from the nonlinear regression are reported in Table S1 of Supporting Information. Figure 2a,b shows the comparisons between experimental and calculated VLE using UNIQUAC activity coefficient model for the binary systems W/AcAc and AcAc/*p*-xyl. Although the fitting of the vapor composition is not excellent in the acetic acid-rich mixture part of the phase diagram, the accuracy of this model for what concerns the pinch point temperatures and compositions is very satisfactory, confirming the thermodynamic approach discussed above. This general result allows us to make a suitable interpretation of our azeotropic distillation column that requires high precision in the critical pure water region rather than a good average fitting in the whole composition of the liquid−vapor diagram. The effectiveness of the proposed method compared to the regression tool available in PRO/II software, which is based on a least-square method (LSA), is highlighted in Table 2, which reports the mean absolute deviation between the experimental data and the calculated ones using the UNIQUAC model with either the robust parameters or the LSA parameters. These are lower for all three components in all the phases. In addition, the same deviation was calculated using the database UNIQUAC parameters, showing that a proper regression algorithm is needed for a good fitting.

A comparison between the experimental VLLE data of the ternary system and the prediction of the model considering interaction parameters estimated with the BzzMath library is shown in Figure 3a,b, where, particularly in the low AcAc concentration zone, both the VLLE and the VLE are in a very good agreement with the experimental data.

5. RESULTS AND DISCUSSION

Two kinds of experiments, for the reason explained above, were conducted: (1) the study of the evaporation curves of three mixtures at different compositions, here discussed, and (2) the use of a micropilot distillation column at different operative conditions, discussed in the following paragraph. All these experimental data were simulated adopting the UNIQUAC activity coefficient model with the optimized parameters to validate, in the experimental conditions, the thermodynamic choices.

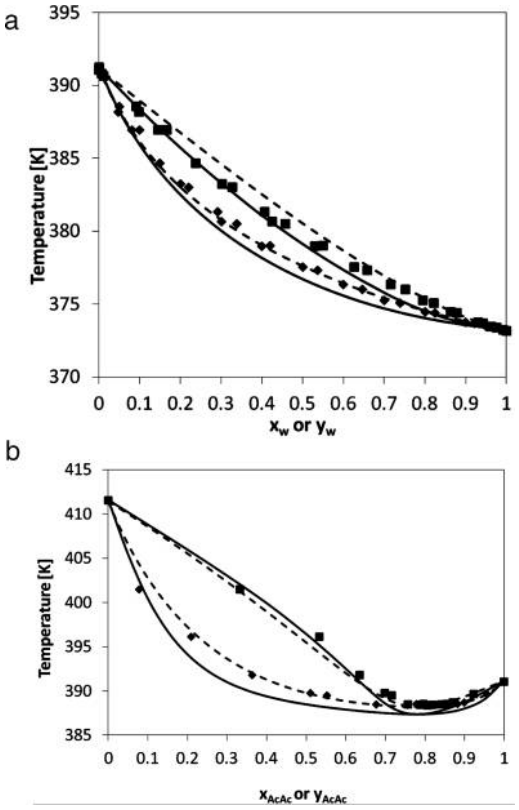

Figure 2. Comparison between experimental (points) and simulated data by UNIQUAC of (a) water/acetic acid system and (b) acetic acid/*p*-xylene system. Dotted line, robust parameter; solid line, LSA parameters.

5.1. Batch Evaporation Curves. The three experimental evaporation curves obtained by loading in the reboiler of the batch distillator three mixtures with different composition, together with the corresponding simulated profiles, are reported in Figure 4a−c.

The initial distillate composition is always addressed to the binary azeotrope W/*p*-xyl having the lower boiling temperature of the system (92 °C). For this reason the distillation curves start from this azeotrope zone of the diagram. Their trends are then addressed to the other parts at a lower temperature of the diagram with a pattern as perpendicular as possible to the isotherms of the system. Being a batch operation, the distillation curves also depend on the relative amounts of the three components that remain in the reboiler, i.e., on the material balance of the components. Moreover, the total composition of the distillate depends at each time on the relative volatility of the different compounds (pure or azeotropic). For this reason, the first isotherm in Figure 4a (which corresponds to the loading mixture $x_W = 0.727$, $x_{AcAc} = 0.182$, and $x_{p\text{-xyl}} = 0.091$, characterized by a low quantity of *p*-xyl) starts with the distillation of the binary W/*p*-xyl azeotrope until the total consumption of the entrainer. After this first step, the W/AcAc mixture remains in the reboiler, not separable, and then we found these two compounds in the distillate together addressed to the "pinch" composition. The

Table 2. Mean Absolute Deviation between VLLE Experimental Data[21] and the Same Calculated with the UNIQUAC Model Using Robust, Nonrobust, and Database Parameters

	aqueous phase			organic phase			vapor phase		
regression algorithm	W	*p*-xyl	AcAc	W	*p*-xyl	AcAc	W	*p*-xyl	AcAc
robust (BzzMath)	0.029	0.005	0.028	0.007	0.029	0.021	0.010	0.021	0.020
PRO/II (LSA)	0.159	0.019	0.140	0.012	0.072	0.060	0.057	0.033	0.090
PRO/II (database)	0.319	0.044	0.275	0.037	0.226	0.187	0.222	0.062	0.145

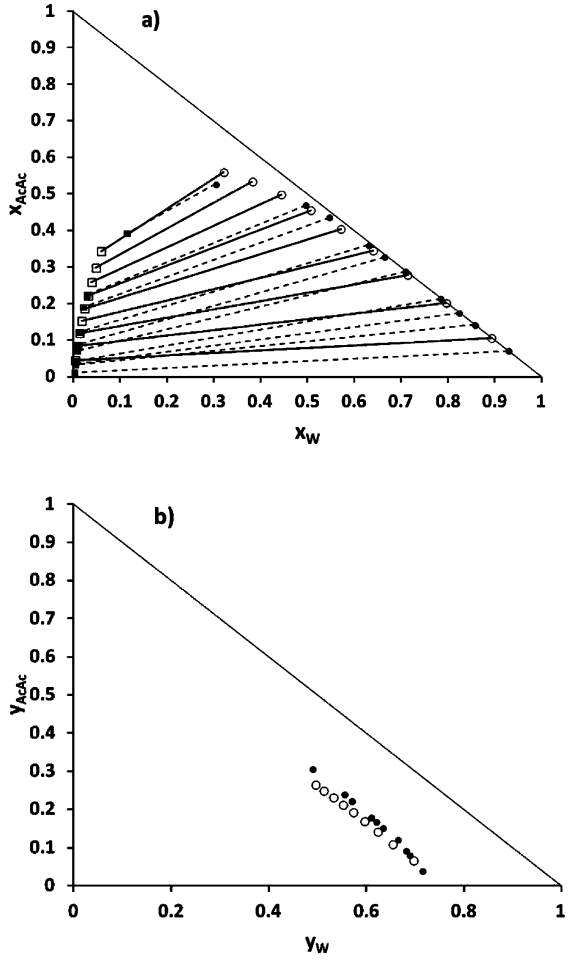

Figure 3. Comparison between experimental (full points and dotted lines) and calculated (empty points and solid lines) using UNIQUAC model with the robust parameter for the W/AcAc/*p*-xyl system. (a) VLLE, liquid compositions, the tie lines are reported for both the data sets; (b) VLLE, vapor compositions.

second isotherm (Figure 4b) (corresponding to the loading mixture $x_W = 0.60$, $x_{AcAc} = 0.10$, and $x_{p\text{-xyl}} = 0.30$) starts in the same way with the distillation of the W/*p*-xyl azeotrope until its composition is allowed from the material balance. The distillation curve is then addressed to the AcAc/*p*-xyl azeotrope, but when the water content is finished, this curve goes toward the binary system AcAc/*p*-xyl. Pure *p*-xyl is obtained when the other components are not present in the reboiler. The last isotherm (Figure 4c, that corresponds to the loading mixture $x_W = 0.40$, $x_{AcAc} = 0.40$, and $x_{p\text{-xyl}} = 0.20$, characterized by a middle quantity of *p*-xyl) is able both to remain in an equilibrium area with all three components and to pass close to the potential hole, corresponding to the azeotrope W/AcAc. The slight difference in temperature between this azeotrope and the pure acetic acid is not sufficient to address this last distillation curve toward the azeotrope. The excellent overlap of both experimental and simulated trends seems to confirm the thermodynamic choice previously discussed.

5.2. Micropilot Continuous Distillation Runs. The different operative parameters and the experimental results for the continuous distillation runs performed on the micropilot column are reported in Table S2 of Supporting Information.

Runs 4 and 5 have been used to estimate the global efficiency of the column. These were performed as follows: the reboiler was loaded with two different mixtures whose composition is $x_W = 0.1$, $x_{AcAc} = 0.1$, and $x_{p\text{-xyl}} = 0.8$ for run 4 and $x_W = 0.1$, $x_{AcAc} = 0.8$, and $x_{p\text{-xyl}} = 0.1$ for run 5. The experimental data shown in Table S2 of Supporting Information were compared with the simulated compositions obtained assuming different total tray efficiencies. The number of trays that minimizes the difference between experimental and simulated data was determined to be equal to eight, corresponding to a mean tray efficiency of 0.53 (8/15), consistent with the presence of a double liquid phase on some trays. For example, the experimental AcAc vapor molar fractions at the 12th tray were 0.062 and 0.104 for run 4 and 5, respectively, whereas the simulated values considering a column with eight theoretical trays were 0.056 and 0.109. This estimation of the total trays of the column agrees with the one determined using a similar column for a different system, i.e., benzene, cyclohexane, sulpholane, and water. This system was characterized by a vapor−liquid−liquid equilibrium in almost all the trays of the column too. On the basis of these results, eight theoretical trays were adopted for simulating all the continuous distillation runs.

Table S2 of Supporting Information shows the results of the four continuous distillation runs 6−9. The lowest amount of AcAc in the distillate was obtained in run 8 ($x_{dist,AcAc} = 0.026$).

In runs 6−8, in the distillate stream, about the same quantity of AcAc is reached. This is because the pinch point, even if it is opened by *p*-xyl, still exists at high concentration of water, as discussed in the next paragraph. Run 9 is characterized, in the distillate stream, by a very high water molar fraction ($x_{dist,W} = 0.55$) because it was performed using the whole column only as stripping section (i.e., both F and Ent were fed at tray number 2).

The lowest amount of water is achieved in run 7, i.e., $x_{res,W} = 0.008$. In this run, there are only two trays in the stripping section and a quantity of entrainer of 42% on molar basis. A low quantity of water in the bottom is reached in run 9, too, in comparison to that of run 7, in which the quantity of *p*-xylene was lower (15% molar) but the number of trays of the stripping section was equal to eight. On the basis of these results, *p*-xylene seems to be a suitable entrainer for W/AcAc separation and its amount is a crucial operative parameter. The optimization of this azeotropic distillation column in terms of economic analysis of the *p*-xyl/F ratio and the amount of W and AcAc in the distillate and residue stream inside the terephthalic acid production process is now in progress and will be reported and discussed in a future paper.

All the experimental runs were simulated on the basis of the thermodynamic model discussed previously, selecting the PRO/

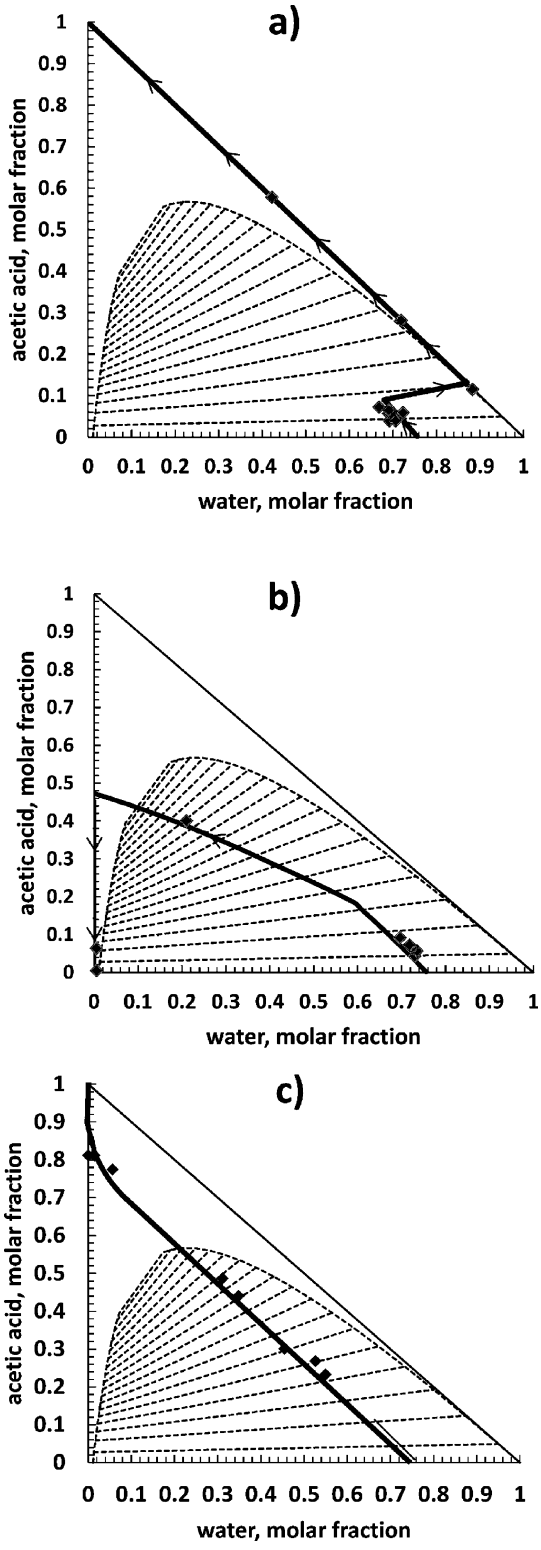

Figure 4. Distillate curve map for the system W/AcAc/*p*-xyl. Comparison between simulated and experimental data for different feeding compositions: (a) $x_w = 0.60$, $x_{AcAc} = 0.10$, $x_{p\text{-xyl}} = 0.30$; (b) $x_w = 0.73$, $x_{AcAc} = 0.18$, $x_{p\text{-xyl}} = 0.09$; and (c) $x_w = 0.40$, $x_{AcAc} = 0.40$, $x_{p\text{-xyl}} = 0.20$.

II CHEMDIST vapor−liquid−liquid algorithm, which is based on the full Newton−Raphson method, and providing both the VLE and VLLE binary interaction parameters reported above. This algorithm is especially suitable for the simulation of highly nonideal chemical systems, and it allows the calculation of two liquid phases on any tray of the column. Equations are solved in a two-step procedure. At first, after initialization, the solver provides a value for the iteration variables. In the second step, tray temperatures along with liquid compositions are employed to perform a flash LLE calculation to assess the presence of liquid phase splitting for each tray. If the second phase occurs, liquid phases are used to calculate new *K*-values with an iterative procedure until convergence. Considering all the streams of the columns, the comparison between all the experimental and the simulated composition of the continuous runs is reported in Figure 5.

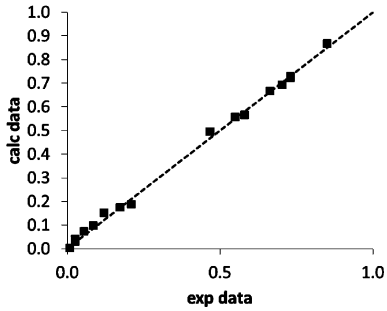

Figure 5. Parity plot between all the experimental and the simulated composition of both distillate and residue of the four continuous distillation runs.

All the points of Figure 5 are close to the diagonal line, i.e., the simulated compositions are satisfactorily similar to the experimental compositions. This result confirms our thermodynamic approach. In Table 1, the normal boiling temperatures and azeotropic compositions of the mixtures AcAc/*p*-xyl and W/*p*-xyl calculated with UNIQUAC model are reported. These values are very close to the experimental values.

To verify the correction estimation of the total tray efficiency, runs 6 and 7 were simulated changing the number of theoretical simulation trays. In both cases, the minimum error between simulated and experimental data was obtained for a number of theoretical simulation trays between eight and nine, confirming the consistency of the value of about 0.5 as total tray efficiency determined as discussed above.

After the experimental verification of the thermodynamic model validity, its isothermal curves have been determined by calculating the boiling point of several mixtures with different composition. The simulated isothermal curves of the W/AcAc/*p*-xyl ternary system are reported in Figure 6.

As expected, when the content of AcAc increases in the mixtures, temperatures increase as well. It is worth noting that there is not inversion of temperature even where the temperature gradient is small according to the experimental observations.

Finally, the positive effect of *p*-xylene on the relative volatility of water and acetic acid is showed in Figure 7, in which the pseudobinary VLE curve is calculated at the pressure of 101.13 kPa for W/AcAc in the presence of 30% molar of *p*-xyl (dotted line).

6. CONCLUSIONS

The choice of UNIQUAC activity coefficient model is suitable for the description of the vapor liquid equilibrium of the involved binary systems and for the vapor−liquid−liquid equilibrium of the ternary system. The robust regression of UNIQUAC binary parameters permitted the comparison of the calculated data with

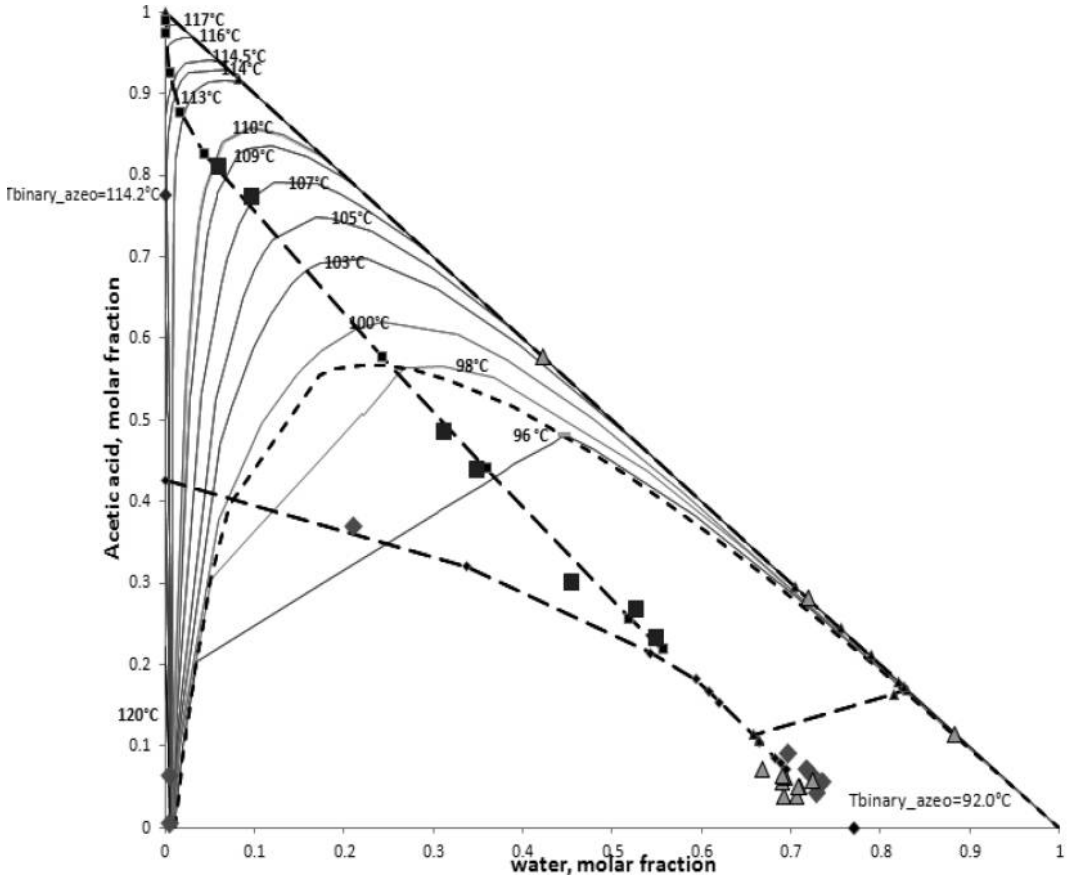

Figure 6. Simulated isothermal curves (using UNIQUAC model) for the W/AcAc/*p*-xyl system. The two binary azeotropes and the three experimental distillation curves are reported too.

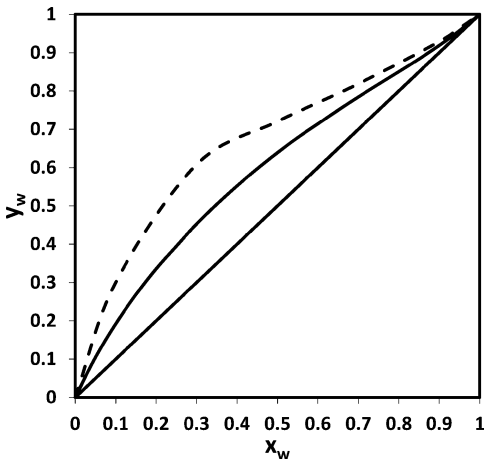

Figure 7. Simulated vapor−liquid equilibrium diagram of the pseudobinary system W/AcAc. The dotted curve is obtained by adding 30% of *p*-xyl on molar basis.

new experimental data from two different appartus, mainly working in the three-phase zone, confirming the correct thermodynamic choices.

An overall tray efficiency of 0.53 was estimated from two specific experimental runs and used in all the simulations of the continuous micropilot column runs. The simulated experimental data confirmed the possibility of designing an extractive column for separating acetic acid from water using *p*-xylene as entrainer. In the specific case of terephthalic acid production, the bottom of the column can be recycled directly to the catalytic reactor without separating *p*-xylene from acetic acid. Because *p*-xylene is a raw material, any contamination by an external substance is avoided.

AUTHOR INFORMATION

Corresponding Author

*Tel.: +39/0250314293. Fax: +39/0250314300. E-mail: carlo.pirola@unimi.it.

Notes

The authors declare no competing financial interest.

ACKNOWLEDGMENTS

Simulation Science Inc. is warmly thanked for the use of PRO/II software version 9.1. The authors thank Prof. Vittorio Ragaini for the helpful discussions and Dr. Ivan Clavenna and Dr. Riccardo Gianola for the experimental work.

REFERENCES

(1) Hindmarsh, E.; Turner, J. A.; Ure, A. M. Process for the production of terephthalic acid. U.S. Patent 5,563,293, October 8, 1996.

(2) Lee, F. M.; Lamshing, W.; Wytcherley, R. M. Method and apparatus for preparing purified terephthalic acid and isophthalic acid from mixed xylenes. U.S. Patent 6,054,610, April 25, 2000.
(3) Lee, H.; Huang, H.; Chien, I. Design and control of an acetic acid dehydration column with *p*-xylene or *m*-xylene feed impurity. 2. Bifurcation analysis and control. *Ind. Eng. Chem. Res.* **2008**, *47*, 3046.
(4) Huang, X. W.; Zhong, W. D.; Qian, F. Thermodynamic Analysis and Process Simulation of an Industrial Acetic Acid Dehydration System via Heterogeneous Azeotropic Distillation. *Ind. Eng. Chem. Res.* **2013**, *52* (8), 2944.
(5) Chien, I. L.; Huang, H.; Gau, T.; Wang, C. Influence of Feed Impurity on the Design and Operation of an Industrial Acetic Acid Dehydration Column. *Ind. Eng. Chem. Res.* **2005**, *44* (10), 3510.
(6) Wilgado, S.; Seider, S. D. Azeotropic distillation. *AIChE J.* **1996**, *42*, 96.
(7) Kiva, V. N.; Hilmen, E. K.; Skogestad, S. Azeotropic phase equilibrium: A survey. *Chem. Eng. Sci.* **2003**, *58*, 1903.
(8) Pham, H. N.; Doherty, M. F. Design and synthesis of heterogeneous azeotropic distillation—III. Column sequences. *Chem. Eng. Sci.* **1990**, *45* (7), 1845.
(9) Siirola, J. J. An industrial perspective on process synthesis. *AIChE J.* **1995**, *91* (304), 222.
(10) Li, C. Dynamic simulation and analysis of industrial purified terephthalic acid solvent dehydration process. *Chin. J. Chem. Eng.* **2011**, *19*, 89.
(11) Tanaka, S.; Yamada, J. Graphical calculation method for minimum reflux ratio in azeotropic distillation. *J. Chem. Eng. Jpn.* **1972**, *5*, 20.
(12) Wasylkiewicz, S. K.; Kobylka, L. C.; Castillo, F. J. L. Optimal design of complex azeotropic distillation columns. *Chem. Eng. J. (Amsterdam, Neth.* **2000**, *79* (3), 219.
(13) Kurooka, T.; Yamashita, Y.; Nishitani, H.; Hashimoto, Y.; Yoshida, M.; Numata, M. Dynamic simulation and nonlinear control system design of a heterogeneous azeotropic distillation column. *Comput. Chem. Eng.* **2000**, *24* (2), 887.
(14) Luyben, M. L.; Tyreus, B. D. An industrial design/control study for the vinyl acetate monomer process. *Comput. Chem. Eng.* **1998**, *22* (7), 867.
(15) Huang, H.; Lee, h.; Gau, T. Design and Control of Acetic Acid Dehydration Column with *p*-Xylene or *m*-Xylene Feed Impurity. 1. Importance of Feed Tray Location on the Process Design. *Ind. Eng. Chem. Res.* **2007**, *46*, 505.
(16) Chien, I. L.; Zeng, K.; Chao, H.; Liu, J. H. Design and control of acetic acid dehydration system via heterogeneous azeotropic distillation. *Chem. Eng. Sci.* **2004**, *59*, 4547.
(17) Wang, S. J.; Huang, K. Design and control of acetic acid dehydratation system via heterogeneous azeotropic distillation using *p*-xylene as an entrainer. *Chem. Eng. Process.* **2012**, *60*, 65.
(18) Pirola, C.; Galli, F.; Bianchi, C. L.; Carvoli, G. Heterogeneous Distillation of the System Water-acetic Acid- P-xylene: Study of Its Fluid Phase Equilibria, Micro-pilot Column Experimental Results and Computer Simulation. *Chem. Eng. Trans.* **2013**, *32*, 1897.
(19) Hayden, J. G.; O'Connel, J. P. A generalized method for predicting second virial coefficients. *Ind. Eng. Chem. Process Des. Dev.* **1975**, *14*, 209.
(20) Abrams, D. S.; Prausnitz, J. M. Statistical Thermodynamics of Liquid Mixtures: A New Expression for the Excess Gibbs Energy of Partly or Completely Miscible Systems. *AIChE J.* **1975**, *21* (1), 116.
(21) Murogova, R. A.; Tudorovskaya, G. L.; Pleskach, N. I.; Safonova, N. A.; Gridin, I. D.; Serafimov, L. A. Dampf fluessing gleichgewichtim system wasser − essigsaeure − p-xylolbei 760 mm Hg. *Zh. Prikl. Khim. (Leningrad)* **1971**, *46*, 2464. (written in Russian).
(22) Perry, R. H.; Green, D. *Perry's Chemical Engineers Handbook*, 6th ed.; McGraw-Hill: New York, 1984.
(23) Buzzi-Ferraris, G.; Manenti, F. BzzMath: Library Overview and Recent Advances in Numerical Methods. *Comput.-Aided Chem. Eng.* **2012**, *30* (2), 1312.
(24) Manenti, F.; Buzzi-Ferraris, G. Criteria for Outliers Detection in Nonlinear Regression Problems, in Computer Aided Chemical Engineering. *Comp.-Aided Chem. Eng.* **2009**, *26*, 913.
(25) Horsely, L. H.; Tamplin, W. S. *Azeotropic Data—II*; Advances in Chemistry Series; American Chemical Society: Washington, DC, 1962.
(26) Ito, T.; Yoshida, F. Vapor-liquid equilibria of water-lower fatty acids systems: Water-formic acid, water-acetic acid and water-propionic acid. *J. Chem. Eng. Data* **1963**, *8* (3), 315.
(27) Marek, J. Vapor-liquid equilibria in mixtures containing an association substance II. Binary mixtures of acetic acid at atmospheric pressure. *Collect. Czech. Chem. Commun.* **1995**, *20*, 1490.
(28) Gmehling, J.; Onken, U. *Vapor-Liquid Equilibrium Collection Data Collection, Aqueous-Organic Systems*; Chemistry Data Series; Dechema: Frankfurt, Germany, 1977; Vol. *1*, Part 1.
(29) Horstmann, S.; Pöpken, T.; Gmehling, J. Phase equilibria and excess properties for binary systems in reactive distillation processes: Part I. Methyl acetate synthesis. *Fluid Phase Equilib.* **2001**, *180*, 221.
(30) Steinigeweg, S.; Gmehling, J. *n*-Butyl Acetate Synthesis via Reactive Distillation: Thermodynamic Aspects, Reaction Kinetics, Pilot-Plant Experiments, and Simulation Studies. *Ind. Eng. Chem. Res.* **2002**, *41*, 5483.
(31) Chengfei, L. Dynamic simulation and analysis of industrial purified terephthalic acid solvent dehydratation process. *Chin. J. Chem. Eng.* **2011**, *19* (1), 89.
(32) Marek, J.; Standart, G. Vapor-Liquid Equilibria in mixtures containing an associating substance. I. Equilibrium relationship for system with an associating component. *Collect. Czech. Chem. Commun.* **1954**, *19*, 1074.
(33) Buzzi-Ferraris, G.; Manenti, F. A Combination of Parallel Computing and Object-Oriented Programming to Improve Optimizer Robustness and Efficiency. *Comput.-Aided Chem. Eng.* **2010**, *28*, 337.
(34) Buzzi-Ferraris, G.; Manenti, F. Kinetic models analysis. *Chem. Eng. Sci.* **2009**, *64*, 1061.
(35) Buzzi-Ferraris, G.; Manenti, F. Outlier Detection in Large Data Sets. *Comput. Chem. Eng.* **2010**, *35*, 388.
(36) Nelder, J. A.; Mead, R. A simplex method for function minimization. *Comput. J.* **1965**, *7*, 308.
(37) Rosenbrock, H. H. An Automatic Method for Finding the Greater or Least Value of a Function. *Comput. J.* **1960**, *3*, 175.
(38) Hooke, R.; Jeeves, T. A. "Direct Search" Solution of Numerical and Statistical Problems. *J. Assoc. Comput. Mach.* **1961**, *8*, 212−229.
(39) Buzzi-Ferraris, G.; Manenti, F. *Nonlinear Systems and Optimization for the Chemical Engineer: Solving Numerical Problems*. Wiley-VCH: Weinheim, Germany, 2014.